Supporting Information

Wei et al. 10.1073/pnas.1321195111

SI Methods

Animal Care. All animal care and use procedures were in accordance with guidelines of the Institutional Animal Care and Use Committee. All experiments were performed with Institute of Cancer Research mice that had been raised for at least two generations in standard conditions to attempt to minimize any intergenerational effects brought about by the animal provider. We generated prediabetes mouse models according to a previous study with slight changes (1). For all comparisons shown, male F_0 founders were weaned from mothers at 3 wk of age, and sibling males were placed into cages with a high-fat diet (HFD; 33% energy as fat) or control diet until 12 wk of age, at which point mice fed with a HFD were injected intraperitoneally with a subdiabetogenic dose of streptozotocin (STZ) (100 mg/kg body weight) and kept on the same diet for 4 wk as described previously (1). Fasting blood glucose (2 h of fasting) was examined each week post-STZ for 4 wk, and only glucose levels at ∼7–11 mM were considered as prediabetes. Females were always raised on standard diet. At 16 wk, male F_0 founders were mated with females. Note that a single male was mated with a single female only once, and thus produced only one litter. Control and prediabetes mating cages were always interspersed with one another. After 1 or 2 d, males were removed, and pregnant females were left alone until their litters were 3 wk of age. Only litter sizes between 8 and 12 were included and litters were standardized to 10 pups at day 1 within father groups to avoid a nutrition imbalance. Paternal prediabetes did not alter litter size or sex ratios in offspring. Note that we always used virgin females to avoid confounding effects brought about by the females. At 3 wk of age a portion of the offspring were killed and islets were generated, each from a different father, which were used for further expression and methylation analysis. Animals were killed between 8:00 AM and 9:00 AM to avoid any mismatches in circadian cycle. Offspring were always raised on standard diet (chow diet) under standard environment conditions. Phenotype data from one offspring per father, chosen at random, were generated at 16 wk of age. Glucose tolerance test (GTT) and insulin tolerance test (ITT) were also performed in offspring at 30 wk of age. For hormonal and metabolic parameters including body weight, weight of white adipose tissue (WAT) and serum biomarkers shown in Table S1, litters from nine control and 10 prediabetic fathers were included, and one offspring per sex per father chosen randomly was used for each test. For other metabolic characteristics, including cumulative weight gain, cumulative energy intake, GTT, and ITT shown in Fig. 1 and Fig. S3, offspring ranging from 5 to 16 were included, depending on the different tests, and also one offspring per sex per father chosen randomly was used for each test. For all comparisons shown in phenotypic and metabolic data, n represents the number of animals used in each test. Blood glucose (Roche Accu-chek), plasma insulin (ALPCO Diagnostic), leptin (ALPCO Diagnostic), triglyceride (Wako Diagnostics), and total cholesterol (Wako Diagnostics) were determined.

GTT and ITT. For GTT, mice were injected intraperitoneally with glucose (2 $g{\cdot}kg^{-1}$) after overnight fasting. Blood glucose was measured at indicated time points. For ITT, we injected insulin (1 $unit{\cdot}kg^{-1}$) intraperitoneally into mice after 2 h of fasting. We collected blood and determined glucose using a glucometer (Roche; Accu-chek). Serum insulin levels were measured using an ELISA kit (ALPCO Diagnostic). Blood glucose or insulin levels were measured before injection (time 0) and at 15, 30, 60, and 120 min after injection. Single time measurements were analyzed by ANOVA, or, if appropriate, by two-tailed Student t test, and time courses were analyzed by repeated-measures ANOVA.

Microarray Expression Profiling. Pancreatic islets were isolated as previously described (2). Total RNA was extracted using TRIzol reagent (Invitrogen). Samples from six control and six prediabetic offspring (three females and three males for each group), each from a different father, were chosen for microarray analysis using NimbleGen Mouse Gene Expression 12× 135K array (Roche NimbleGen), according to the manufacturer's instructions. A series of software (NimbleScan software and Agilent GeneSpring GX software) was used for data analysis. All array data and additional details on samples and analysis are available on GEO under accession no. GSE43239. Gene expression levels were compared using one-way ANOVA. Probes with fold change of >2 and significant difference ($P < 0.05$) were chosen for further analysis. Differentially expressed genes were hierarchically clustered using Cluster 3.0.

qRT-PCR. We analyzed mRNA levels by qRT-RCR after reverse transcription as described before (3). The same samples used for microarray analysis (one offspring per father; $n = 6$, prediabetes; $n = 6$, control) were used for qRT-PCR. Total RNA was extracted from the pancreatic islets using TRIzol reagent (Invitrogen) and quantified by absorbance at 260 nm and 280 nm in a PerkinElmer spectrophotometer. It was then used as a template for cDNA synthesis by SuperScript III first-strand synthesis (Invitrogen) with random hexamers. mRNA quantity was determined with the quantitative RT-PCR 7500 system (Applied Biosystems), using primer sequences summarized in Dataset S5 and SYBR Green SuperMix UDG (Invitrogen). PCR was performed in a final volume of 25 μL, consisting of diluted cDNA sample, 1× SYBR Green Mix (Invitrogen), primers optimized for each target gene, and nuclease-free water. The PCR condition was 40 cycles at 95 °C for 30 s and 55 °C for 1 min and 72 °C for 30 s. Gene transcript levels were normalized to the housekeeping gene *Gapdh* (for *Pik3r1* and *Ptpn1*) or *β-Actin* (for *Pik3ca* and *Pfk*). The experiments were conducted in triplicate for each gene in each sample, and the results were expressed as $2^{-(\text{target gene number of cycles} - \textit{Gapdh/β-Actin} \text{ number of cycles})}$.

Sperm Isolation. Caudal epididymis was dissected from killed mice, punctured, and incubated for 30 min in M2 media at 37 °C. Supernatant was removed, centrifuged (3000 × g for 5 min), washed twice in PBS and once in water, and incubated in cell lysis buffer. Sperm preparations were assayed for purity by microscopy. Sperm nuclei were stained with DAPI for 10 min, and five fields for each sample were randomly selected for the analysis. All nuclei displayed typical sperm morphology (like a tadpole), which was important to rule out the possibility of contamination by somatic cells.

Methylated DNA Immunoprecipitaton Sequencing and Methylated DNA Immunoprecipitation-qPCR. For offspring, the same animals used in microarray analysis were used for the methylated DNA immunoprecipitaton (MeDIP) study. For sperm, the animals used were exactly the fathers of offspring used for microarray analysis. The MeDIP method was adapted from a previous study (4). Four micrograms of purified genomic DNA was fragmented to a size of ∼100–500 bp using a Covaris machine. After denaturation, the DNA was immunoprecipitated with 10 μg of monoclonal anti-

body against 5-methylcytidine (Diagenod) in 300 μL IP buffer (10 mM sodium phosphate at pH 7.0, 140 mM NaCl, 0.05% Triton X-100) for 5 h at 4 °C and then washed three times with 800 μL IP buffer. Immunoprecipitated DNA was recovered with proteinase K digestion followed by column-based purification (DNA Wizard; Promega). Recovered material was Solexa sequenced, with ∼49 million uniquely mappable reads per library. All MeDIP sequencing (Seq) data and additional details on samples and analysis are available on GEO under accession number GSE43239. For qPCR following MeDIP, methylation levels of the randomly selected 10 regions (five down-regulated and five up-regulated) distributed on different chromosomes that were most affected by paternal prediabetes in both sperm and offspring were examined. Recovered DNA fractions were diluted 1/50 and measured using real-time PCR with an Applied Biosystems 7500 system and SYBR Green SuperMix UDG (Invitrogen). The promoter of *H19* gene was used for normalization. Primers are summarized in Dataset S5 and the regions that are examined are as follows:

Sperm regions 1–10 (related to Fig. 6*B*) are 1, Chr2:153,237,362–153,237,522; 2, Chr7:109,600,912–109,601,125; 3, Chr6:101,120,683–101,120,891; 4, Chr9:123,370,955–123,371,154; 5, Chr11:60,649,983–60,650,202; 6, Chr15:57,251,379–57,251,588; 7, Chr1:112,834,213–112,834,388; 8, Chr13:34,160,377–34,160,525; 9, Chr5:43,946,470–43,946,657; 10, Chr19:50,702,583–50,702,841.

Islet regions 1–10 (related to Fig. 5*B* and Fig. 6*D*) are 1, Chr17:17,262,800–17,262,954; 2, Chr7:38,968,318–38,968,524; 3, Chr11:52,222,933–52,223,104; 4, Chr4:120,085,995–120,086,226; 5, Chr10:62,711,197–62,711,464; 6, Chr14:118,063,774–118,063,947; 7, Chr2:166,637,398–166,637,634; 8, Chr1:17,726,053–17,726,240; 9, Chr9:21,990,614–21,990,849; 10, Chr15:98,036,836–98,037,039.

Liver regions (related to Fig. S6) are *Aurkc*, Chr7:6,948,943–6,949,168; *Casr*, Chr16:36,562,541–36,562,717; *Atg4c*, Chr4:98,868,359–98,868,488; *Esco1*, Chr18:10,606,679–10,606,891; *Suds3*, Chr5:117,567,141–117,567,368; *Camk1d*, Chr2:5,213,394–5,213,633; *Rpl27*, Chr11:101,306,427–101,306,652; *Bzw2*, Chr12:36,828,214–36,828,365.

Bisulfite Sequencing. Bisulfite genomic sequencing was performed as previously described (3). Bisulfite modification was accomplished using the EZ DNA Methylation kit (Zymo Research). The converted DNA was then amplified by PCR with primer sequences summarized in Dataset S5. The obtained PCR products were purified using Min Elute Gel Extraction kit (Invitrogen) and cloned into the pMD18-T Vector (Takara). Individual clones were grown and the plasmids were purified using PureLink Miniprep kit (Invitrogen). The positive clones were confirmed by PCR and ∼15 clones for each subject were sequenced using an automatic sequencer (ABI PRISM-77). For offspring, the same samples that were used in microarray were used for bisulfite sequencing. For sperm, the animals used were exactly the fathers of offspring used for microarray analysis. For bisulfite sequencing, pooled DNA of six animals (equally from each animal) for each group was used for analysis. Embryos of E3.5 blastocysts were obtained by natural breeding. Estrous females were mated with males, and the morning of the vaginal plug was designated E0.5. Blastocysts were collected at E3.5 by flushing the oviducts with M2 medium. Each bisulfite treatment was performed on 18 pooled blastocysts derived from three animals (six blastocysts randomly selected from each animal) for each group. The regions that are examined by bisulfite sequencing are as follows: *Pik3ca*, Chr3:32,356,060–32,356,676; *Pik3r1*, chr13:102,472,126–102,472,674; *Ptpn1*, chr2:167,774,077–167,774,396. It should be noted that, because the unmethylated 5-hydroxymethyl cytosine was also converted into uracil during bisulfite treatment, the results represent pooled status of 5-methyl cytosine and 5-hydroxymethyl cytosine.

Western Blot. Sperm samples were collected from STZ-alone–treated nondiabetic mice at 1 d, 1 wk, and 4 wk post-STZ injection. Sperm samples were also collected from normal mice and subjected to a 3-min UV (50J) exposure. For each group, three mice selected randomly were included. Western blot was performed as described previously (3). Sperm extracts were prepared by sonicating samples in lysis buffer containing 50 mM Tris (pH 7.9), 150 mM NaCl, 1 mM EDTA, 20% Triton X-100, proteinase inhibitor mixture (Roche Applied Sciences), and halt phosphatase inhibitor mixture (Pierce). For Western blot analysis, protein lysates were diluted to 2 μg/μL to standardize protein loading. A total of 40 μg of protein extracts was loaded onto the polyacrylamide gel and separated by electrophoresis. Proteins were transferred to polyvinylidene fluoride membranes and the membranes were then incubated in blocking buffer at 4 °C overnight. Blots were incubated with γH2AX (phosphorylated Ser139, Bioworld, 1:200) or β-actin (Santa Cruz Biotechnology; 1:1,000) primary antibody and horseradish peroxidase-conjugated IgG (Santa Cruz Biotechnology; 1:1,000) secondary antibody. The image was captured and analyzed with the enhanced chemiluminescence detection system (Amersham).

STZ-Alone–Treated Nondiabetic Model. An identical amount of STZ was injected in chow-fed mice at 12 wk of age, and fasting blood glucose (2 h of fasting) was examined each week post-STZ for 4 wk. Only glucose levels less than 5 mM were considered as an STZ-alone–treated nondiabetic model. Mating was done as described for prediabetes mice, and islets of offspring at 3 wk of age were isolated and used for further analysis.

Statistical Analyses. Phenotype data were analyzed by SPSS 16.0 after log transformation or square-root transformation unless raw data were normally distributed. Measurements at single time points were analyzed by ANOVA, or, if appropriate, by two-tailed Student *t* test. Time courses were analyzed by repeated-measurements ANOVA. All data are shown as mean ± SEM; $P < 0.05$ was considered statistically significant.

SI Discussion

It is well known that humans with impaired fasting glucose and impaired glucose tolerance exhibit marked defects in β-cell function (5, 6). Our results show that pancreatic islets isolated from offspring of prediabetic fathers also exhibit multiple alterations in gene expression. Specifically, some of these changes involve a number of genes demonstrated to affect β-cell function, that is, *Hnf1a*, *Pfk*, *Hif3a*, and several genes involved in the insulin signaling pathway (including *Pik3ca*, *Pik3r1*, and *Ptpn1*). Studies in knockout mice show that decreased levels of these genes can lead to altered glucose sensing and defects in insulin sensitivity (7–9), and therefore these molecular findings are correlated with glucose intolerance and insulin insensitivity observed in offspring. Combined with studies showing that offspring glucose levels are affected by paternal fasting (10), these data demonstrate that paternal physiological conditions have broad effects on the metabolism of offspring. Interestingly, a study from Carone et al. reported that exposure of male mice to low-protein diet was associated with elevated hepatic expression of lipid biosynthetic genes in offspring (11). Therefore, transgenerational effects may be sensitive to certain pathways representing environmental conditions that had been experienced by the father. It will be interesting in the near future to compare the transgenerational effects contributed by fathers in different physiological conditions. The reprogrammed gene expression state is most likely affected by epigenetic modifications. Our genome-wide analyses of cytosine methylation in the pancreatic islets of offspring identified several insulin signaling-associated genes, which were differentially methylated depending on paternal prediabetes. Notably, the major enzymes involved

in the insulin signaling pathway, *Pik3ca* and *Pik3r1*, exhibited higher methylation in offspring of prediabetic fathers. Furthermore, *Ptpn1*, a tyrosine phosphatase that has been shown to be a negative regulator of insulin sensitivity, exhibited lower methylation in offspring of prediabetic fathers. These facts lead to the hypothesis that epigenetic regulation is an upstream event that affects the entire gene expression status.

In our study, we found that a significant number of differentially methylated genes in sperm overlapped with that of islets. An interesting question is whether paternal metabolic state induced methylation changes in sperm-inherited genes can also be inherited to other somatic tissues. To address this issue, we examined methylation levels of the sperm-inherited genes in the liver of offspring, which is the primary site of insulin action and is also critical for the regulation of glucose metabolism. We randomly selected eight genes (four up-regulated, Fig. S7 *A–D*; four down-regulated, Fig. S7 *E–H*) distributed on different chromosomes whose methylation status can be inherited from sperm to islets from the MeDIP-Seq data. MeDIP-qPCR analysis showed that of the eight genes analyzed, three of them (one up-regulated, Fig. S7*C*; two down-regulated, Fig. S7 *F* and *H*) showed similar methylation differences as seen in islets, and the remaining five genes exhibited no alterations in methylation levels between prediabetes and control groups (Fig. S7 *A*, *B*, *D*, *E*, and *G*). These results indicate that for certain genes or regions, the cytosine methylation in sperm is possible to inherit to other somatic tissues, whereas for other genes or regions, the cytosine methylation in somatic tissues may be largely affected or established during some point of development. Whether environmentally induced cytosine methylation changes in sperm-inherited genes can be inherited to other somatic tissues is an open question. It will be interesting in the near future to compare the cytosine methylation pattern changes of sperm with that of different somatic tissues.

Our findings may have wider implications, as we provided molecular evidence for the environmental inheritance or the inheritance of acquired characteristics. Environmentally induced paternal metabolic changes affect epigenetic marks and can be inherited for several generations. These findings may have implications in explaining the prevalence of obesity, type 2 diabetes, and other chronic metabolic diseases. The findings may be an important step in understanding environmental inheritance.

1. Luo J, et al. (1998) Nongenetic mouse models of non-insulin-dependent diabetes mellitus. *Metabolism* 47(6):663–668.
2. Kulkarni RN, et al. (1999) Altered function of insulin receptor substrate-1-deficient mouse islets and cultured beta-cell lines. *J Clin Invest* 104(12):R69–R75.
3. Wei Y, et al. (2011) Unfaithful maintenance of methylation imprints due to loss of maternal nuclear Dnmt1 during somatic cell nuclear transfer. *PLoS ONE* 6(5):e20154.
4. Weber M, et al. (2007) Distribution, silencing potential and evolutionary impact of promoter DNA methylation in the human genome. *Nat Genet* 39(4):457–466.
5. Butler AE, et al. (2003) Beta-cell deficit and increased beta-cell apoptosis in humans with type 2 diabetes. *Diabetes* 52(1):102–110.
6. Gerich JE (1998) The genetic basis of type 2 diabetes mellitus: Impaired insulin secretion versus impaired insulin sensitivity. *Endocr Rev* 19(4):491–503.
7. Bell GI, Polonsky KS (2001) Diabetes mellitus and genetically programmed defects in beta-cell function. *Nature* 414(6865):788–791.
8. Froguel P, Velho G (2001) Genetic determinants of type 2 diabetes. *Recent Prog Horm Res* 56:91–105.
9. Kewley RJ, Whitelaw ML, Chapman-Smith A (2004) The mammalian basic helix-loop-helix/PAS family of transcriptional regulators. *Int J Biochem Cell Biol* 36(2):189–204.
10. Anderson LM, et al. (2006) Preconceptional fasting of fathers alters serum glucose in offspring of mice. *Nutrition* 22(3):327–331.
11. Carone BR, et al. (2010) Paternally induced transgenerational environmental reprogramming of metabolic gene expression in mammals. *Cell* 143(7):1084–1096.

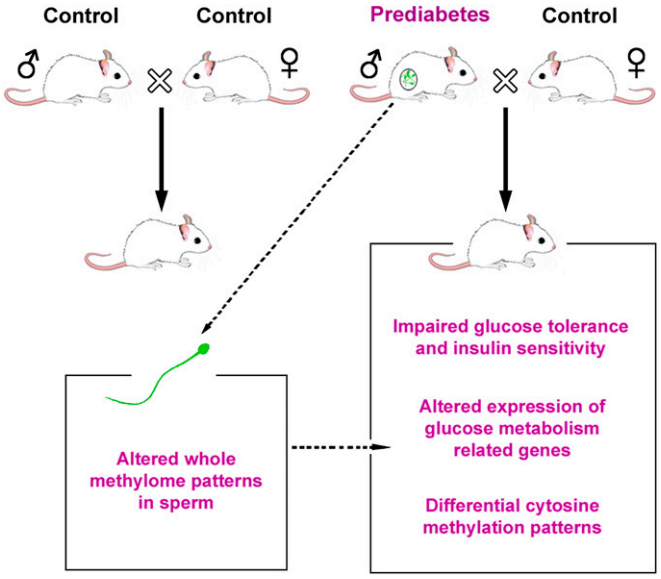

Fig. S1. Experimental schematic. Control or prediabetic males were mated with females. Offspring of prediabetic fathers exhibited impaired glucose tolerance and insulin insensitivity. Gene expression profiling reveals altered expression of genes involved in glucose metabolism. Consistently, differential methylation patterns were observed in offspring of prediabetic fathers. A paternal prediabetes altered overall methylome patterns in sperm, which contributed largely to the metabolic and epigenetic changes in offspring.

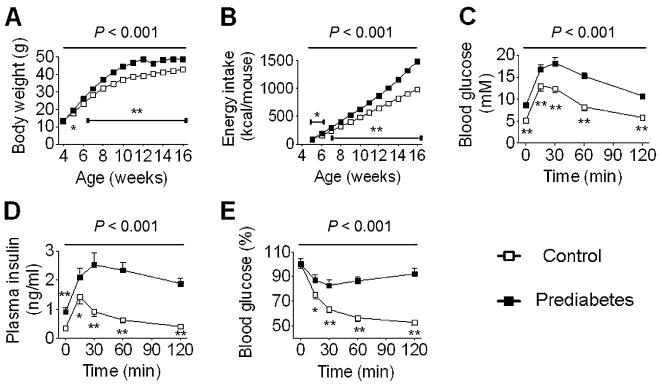

Fig. S2. Prediabetic fathers exhibit adiposity, glucose intolerance, and insulin resistance. (*A*) Body weight trajectories (control, prediabetes: $n = 14$ and 15, respectively). (*B*) Cumulative energy intake ($n = 5$ and 6, respectively). (*C*) Blood glucose during GTT ($n = 7$ and 6, respectively). (*D*) Plasma insulin during GTT ($n = 7$ and 6, respectively). (*E*) Blood glucose during ITT ($n = 8$ and 8, respectively). Data are expressed as mean ± SEM; $*P < 0.05$, $**P < 0.01$, versus control. *P* values for significance between groups in repeated-measure analysis are shown (*Upper*).

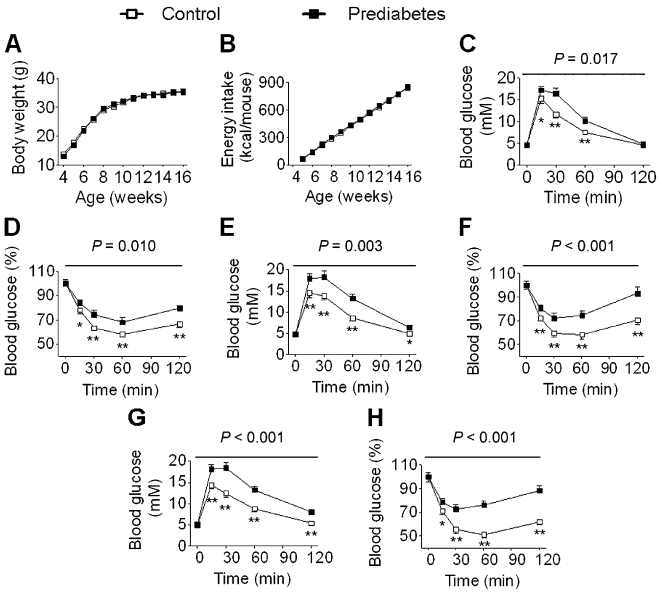

Fig. S3. Paternal prediabetes leads to glucose intolerance and insulin insensitivity in female offspring at 16 wk and 30 wk and male offspring at 30 wk. (*A*) Body weight trajectories in female offspring (control, prediabetes: $n = 12$ and 15, respectively). (*B*) Cumulative energy intake in female offspring ($n = 6$ and 5, respectively). (*C*) Blood glucose of female offspring during GTT at 16 wk ($n = 8$ and 8, respectively). (*D*) Blood glucose of female offspring during ITT at 16 wk ($n = 9$ and 7, respectively). (*E*) Blood glucose of female offspring during GTT at 30 wk ($n = 8$ and 6, respectively). (*F*) Blood glucose during ITT of female offspring at 30 wk ($n = 9$ and 8, respectively). (*G*) Blood glucose during GTT of male offspring at 30 wk ($n = 7$ and 9, respectively). (*H*) Blood glucose during ITT of male offspring at 30 wk ($n = 9$ and 9, respectively). Data are expressed as mean ± SEM; $*P < 0.05$, $**P < 0.01$, versus control. *P* values for significance between groups in repeated-measure analysis are shown (*Upper*).

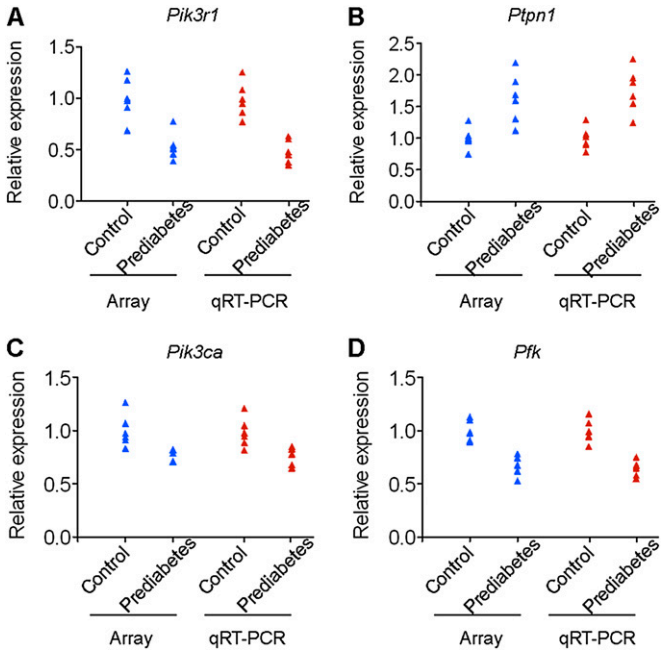

Fig. S4. Validation of microarray data by qRT-PCR. Quantitative RT-PCR was used to determine levels of *Pik3r1* (*A*) and *Ptpn1* (*B*) relative to the control gene *Gapdh*, which showed no change in the microarray dataset. To further confirm the microarray data, quantitative RT-PCR was performed on *Pik3ca* (*C*) and *Pfk* (*D*) relative to another housekeeping gene, *β-actin*, which also showed no change in the microarray dataset. Animals are grouped by paternal phenotype and by the examined method, and data are expressed as ΔC_T between the examined gene and the housekeeping gene, normalized relative to the average of control animals.

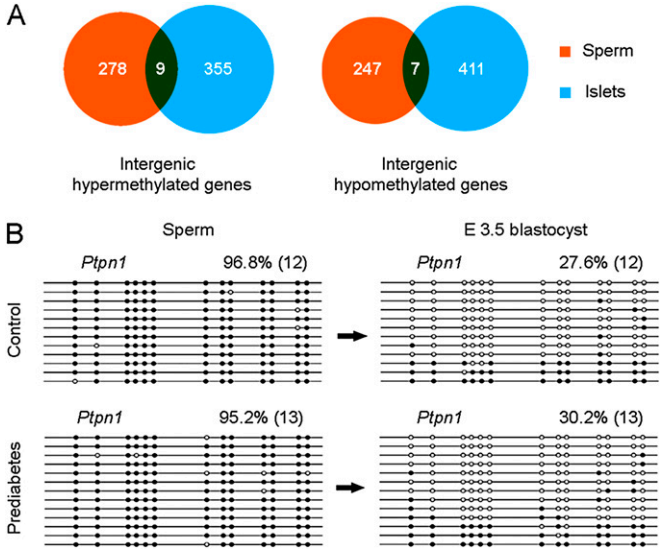

Fig. S5. Effects of paternal prediabetes on methylation of intergenic regions and *Ptpn1* gene. (*A*) Venn diagrams of differentially methylated intergenic element-associated genes show only a small number of overlaps between sperm and pancreatic islets. (*B*) Bisulfite sequencing of *Ptpn1* in sperm and E3.5 blastocysts shows no change of DNA methylation between control and prediabetes groups, indicating that the differential methylation status observed in offspring is established at some point during development. The gene is shown above the graphs. White circles represent unmethylated CpGs, and black circles represent methylated CpGs. Values on each bisulfite grouping indicate the percentage of CpG methylation, with number of analyzed clones in parentheses.

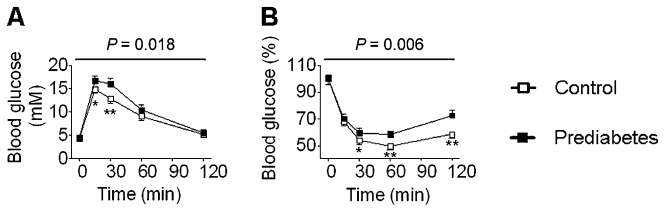

Fig. S6. Paternal prediabetes leads to impaired glucose tolerance and insulin sensitivity in the F_2 generation females. (*A*) Blood glucose during GTT at 16 wk of F_2 generation females ($n = 8$ and 7, respectively). (*B*) Blood glucose during ITT at 16 wk of F_2 generation females ($n = 8$ and 7, respectively). Data are expressed as mean ± SEM; $*P < 0.05$, $**P < 0.01$, versus control. *P* values for significance between groups in repeated-measure analysis are shown (*Upper*).

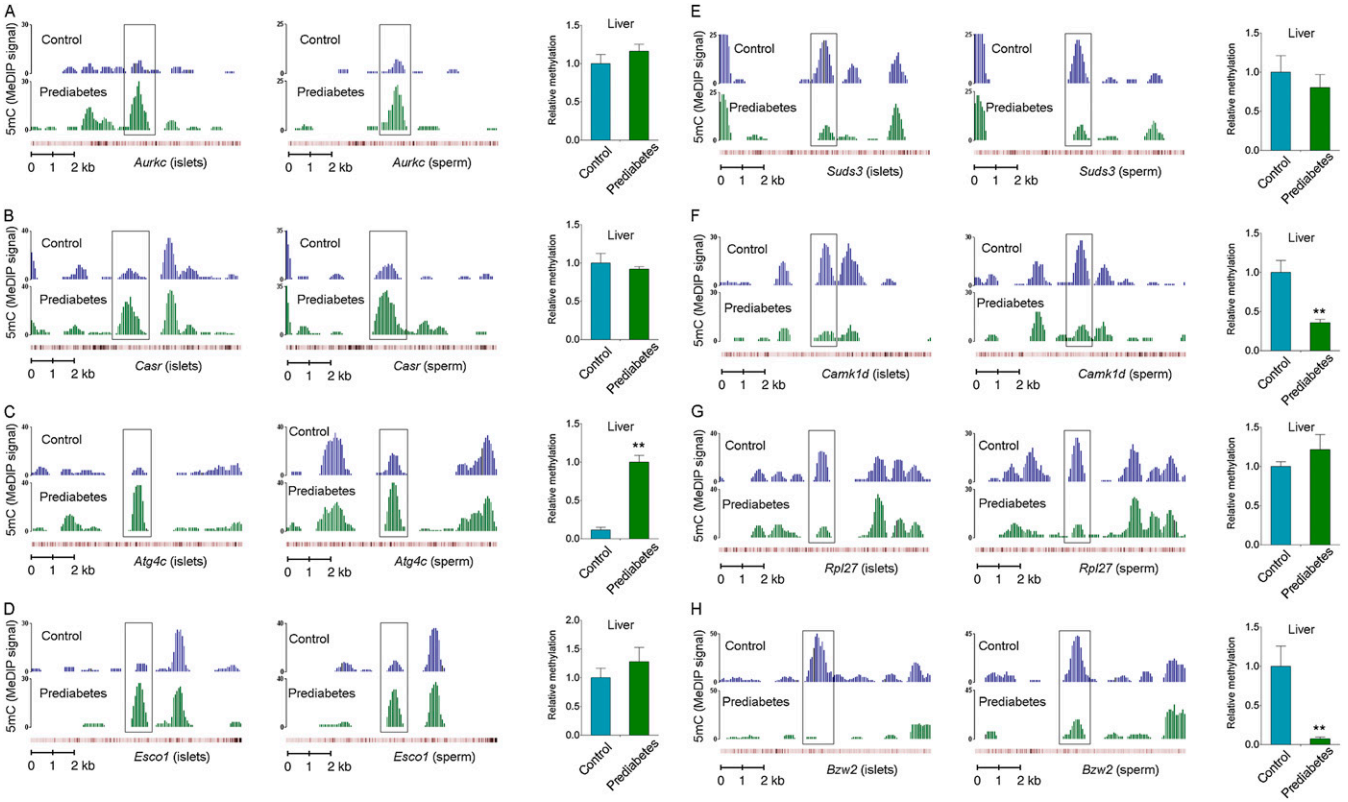

Fig. S7. Effects of paternal prediabetes on methylation levels of sperm-inherited genes (seen in islets) in the liver of offspring. MeDIP-qPCR for methylation levels of the randomly selected four up-regulated regions (*A–D*) and four down-regulated regions (*E–H*) distributed on different chromosomes whose methylation status can be inherited from sperm to islets in the liver of offspring. Methylation levels of the indicated regions were normalized to the promoter of *H19* gene, which showed no change in the MeDIP-Seq dataset. For each panel, the chromatogram shows smoothed number of normalized reads in islets (*Left*) and sperm (*Center*), which represent output MeDIP signals, and the histogram (*Right*) shows the relative methylation levels for indicated genes in the liver of offspring. Genes are shown below the chromatogram, and red bars represent the position of the CpGs. The regions that are differentially methylated and inherited from sperm to islets are shown in the box. It should be noted that, in the case of *Atg4c* as shown in *C*, because the qPCR signals were very weak in the control group, we set the average methylation level of prediabetes animals as 1. All of the detailed region information is described in *SI Methods*.

Table S1. Hormonal and metabolic parameters in fathers and offspring

Group and parameter	Control	Prediabetes	*P* value
Fathers	$n = 9$	$n = 10$	
Body weight, g	43.0 ± 0.7	48.8 ± 0.8	<0.001
Mesenteric WAT, g	1.52 ± 0.07	2.91 ± 0.12	<0.001
Retroperitoneal WAT, g	1.39 ± 0.08	2.59 ± 0.10	<0.001
Gonadal WAT, g	1.85 ± 0.05	3.15 ± 0.19	<0.001
Sum of WAT, g	4.75 ± 0.07	8.66 ± 0.23	<0.001
Total cholesterol, mM	2.11 ± 0.08	2.58 ± 0.13	0.012
Triglyceride, mM	0.78 ± 0.07	1.26 ± 0.07	<0.001
Glucose, mM	4.65 ± 0.15	9.04 ± 0.31	<0.001
Leptin, ng/mL	1.84 ± 0.11	5.16 ± 0.40	<0.001
Insulin, ng/mL	0.35 ± 0.03	0.91 ± 0.06	<0.001
HOMA-IR	1.55 ± 0.15	7.84 ± 0.69	<0.001
Male offspring	$n = 9$	$n = 10$	
Body weight, g	42.0 ± 0.9	42.5 ± 1.0	0.70
Mesenteric WAT, g	1.53 ± 0.08	1.60 ± 0.08	0.56
Retroperitoneal WAT, g	1.36 ± 0.09	1.30 ± 0.07	0.61
Gonadal WAT, g	1.87 ± 0.09	1.90 ± 0.11	0.82
Sum of WAT, g	4.76 ± 0.12	4.80 ± 0.16	0.83
Total cholesterol, mM	2.12 ± 0.09	2.31 ± 0.10	0.19
Triglyceride, mM	0.80 ± 0.07	0.91 ± 0.06	0.25
Glucose, mM	4.56 ± 0.15	4.83 ± 0.10	0.14
Leptin, ng/mL	2.04 ± 0.19	2.51 ± 0.18	0.06
Insulin, ng/mL	0.36 ± 0.01	0.41 ± 0.02	0.07
HOMA-IR	1.57 ± 0.11	1.89 ± 0.13	0.08
Female offspring	$n = 9$	$n = 10$	
Body weight, g	35.6 ± 1.3	35.5 ± 1.3	0.94
Mesenteric WAT, g	1.31 ± 0.05	1.35 ± 0.10	0.73
Retroperitoneal WAT, g	0.88 ± 0.03	0.87 ± 0.07	0.91
Gonadal WAT, g	2.06 ± 0.12	2.08 ± 0.06	0.85
Sum of WAT, g	4.25 ± 0.23	4.30 ± 0.16	0.80
Total cholesterol, mM	2.44 ± 0.14	2.37 ± 0.15	0.88
Triglyceride, mM	0.73 ± 0.05	0.73 ± 0.04	0.99
Glucose, mM	4.52 ± 0.12	4.67 ± 0.14	0.47
Leptin, ng/mL	2.17 ± 0.06	2.33 ± 0.13	0.18
Insulin, ng/mL	0.32 ± 0.01	0.36 ± 0.03	0.09
HOMA-IR	1.38 ± 0.06	1.58 ± 0.09	0.16

WAT, white adipose tissue.

Other Supporting Information Files

Dataset S1 (XLS)
Dataset S2 (XLS)
Dataset S3 (XLS)
Dataset S4 (XLS)
Dataset S5 (XLS)